Numerical Analysis of Secondary Motion of Piston Skirt in Engines

Sunny Narayan

Mechanical Engineering Department, Qassim University, Saudi Arabia, 51431.

Vipul Gupta

Mechanical Engineering Department, Indus University, India, 174301.

(Received 4 May 2018; accepted 23 July 2018)

The motion of the piston pin plays an important role in the secondary motion of the skirt, and in the resulting noise and vibration features of combustion engines. In the engine, the small gap between the piston skirt and the cylinder liner allows a small movement of the piston in a lateral direction, in addition to the reciprocating motion of the piston during operation of the engine. Although the piston is held in its cylinder bore by means of piston rings, there is a small gap between the rings and the grooves, and hence it is free to move within this gap. The existence of the piston-liner gap puts a limit on the amplitude of piston motion, but not on the degree of freedom in the lateral, as well as the reciprocating, motion.

This work discusses a numerical model of the lateral motion of the skirt. Dynamic parameters of the skirt were used to analyse this motion. Further, COMSOL-7 Multiphysics was used to simulate the motion of the skirt. Both the simulation and the experiment showed a good correlation.

NOMENCLATURE

F_x	Piston side-thrust force
ω	Angular velocity
M	Mechanical mobility
m_p	Dynamic mass of piston assembly
m_b	Dynamic mass of engine block
I_p	Moment of inertia piston assembly
θ''	Rotatory acceleration of piston assembly
θ'	Rotatory velocity of piston assembly
θ	Tilting angle of piston
K_p	Dynamic stiffness of piston assembly
K_b	Dynamic stiffness of engine block
C_p	Dynamic damping coefficient of piston assembly
C_b	Dynamic damping coefficient of engine block
C_C	Dynamic contact damping coefficient of assembly
K_C	Dynamic contact stiffness of assembly
C_θ	Dynamic torsional damping coefficient of piston
K_θ	Dynamic torsional stiffness of piston
$C_{C\theta}$	Dynamic torsional contact damping coefficient of piston
$K_{C\theta}$	Dynamic torsional contact stiffness of piston
X_p''	Piston assembly lateral acceleration
X_p'	Piston assembly lateral velocity
X_p	Piston assembly lateral displacement
X_b''	Block assembly lateral acceleration
X_b'	Block assembly lateral velocity
X_b	Block lateral displacement
M_z	Moment about piston pin
X_c	Piston-liner gap

1. INTRODUCTION

Noise emissions from an internal combustion engine can be classified as combustion-based noise, mechanical noise, aerodynamic flow noise, etc. There is a small lateral gap between the skirt and the liner due to manufacturing tolerances. Hence, the skirt is able to strike the liner in a lateral direction, in addition to its usual reciprocating motion. This lateral motion of the skirt is also known as its slapping motion. Several numerical models have been studied in the past to analyse this secondary motion of the skirt.[1] These models have taken dynamics and tribological analysis into account. However, effects of damping have been neglected in past research works.[2–5] During analysis of lateral contact of the liner with the skirt, various dynamic parameters need to be taken into account. Different methods to control the piston slapping motion includes optimization of skirt design parameters like piston pin offset, skirt stiffness, clearance size, and skirt profile. However, there is a trade-off between these parameters. As an example, reduction of the lateral gap between the skirt and the liner reduces the lateral motion of skirt, but at the same time, it increases frictional forces. Other alternative methods have been explored, including the use of dampers to reduce energy in the skirt-liner system.[6–8]

The piston secondary motion is crucial to understand the various frictional forces in piston assembly, which contribute to 30–40% of total mechanical losses, and hence are a major cause of inefficiency in an engine.[9–11] The piston translates from one side, to the liner, to the other side, due to the change in direction of the side-thrust force and due to the motion of connecting rod.[12–15]

The basic motion of the piston's secondary motion can be seen in Fig. 1. A numerical model shown in Fig. 1 was used to analyse this motion. The dynamic motion of the skirt may be summarized in matrix form as given by Eq. (1).[1]

$$\begin{bmatrix} m_{piston}\left(1-\frac{b_c}{L}\right)+m_{pin}\left(1-\frac{a_p}{L}\right) & m_{piston}\left(\frac{b_c}{L}\right)+m_{pin}\left(\frac{a_p}{L}\right) \\ m_{piston}\left(1-\frac{a_p}{L}\right)(b_c-a_p)+m_{piston}\left(\frac{I_p}{L}\right) & m_{piston}\left(\frac{a_p}{L}\right)(b_c-a_p)-m_{piston}\left(\frac{I_p}{L}\right) \end{bmatrix} \begin{bmatrix} e_t'' \\ e_b'' \end{bmatrix} = \begin{bmatrix} F_h-(F_{IC}+F_g+F_f)\tan\phi \\ F_{IC}^{-}(a_p-b_c)+F_gC_p+F_{IC}C_g+M_h+M_f \end{bmatrix}. \quad (1)$$

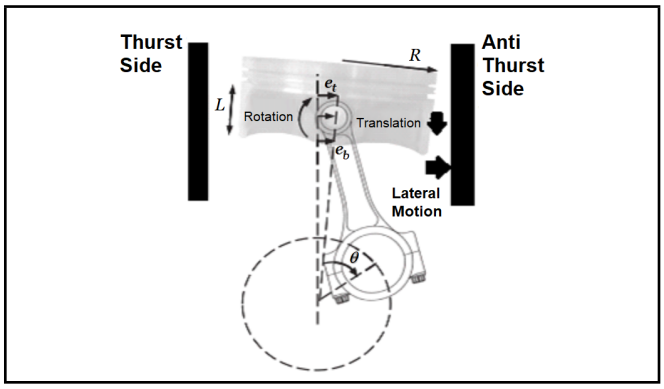

Figure 1. Basic model of piston secondary motion.[1]

2. BACKGROUND

The reciprocating primary motion of pistons in the model, which is determined by the pressure of combustion gas acting on top of the skirt, has been studied by McFadden et al.[16] and Geng et al.[17] Several simulations have been carried out to study the two-dimensional model of piston slap.[18–20] Various parameters considered include centre of gravity offset,[21] skirt profile,[22] effects of variable inertial force,[23] effects of frictional force,[24] and effects of lubricating oil.[25]

McNally developed a numerical method to analyse piston motion, assuming that the skirt is a rigid body.[26] Livanos et al. studied effects of friction on the piston motion of a marine diesel engine.[27] The effects of engine speed and load were analysed and compared with empirical results. Mansouri et al. validated a numerical model of a skirt, considering the roughness and topology of the skirt.[28] They developed various correlations and scaling laws that could be used for qualitative design of skirts. Lu et al. used the Jakobson-Floberg-Olsson (JFO) condition to study the rupture and reformation of an oil film.[29] Gunelsu et al. used a Broyden's scheme-based iteration phase method to analyse metal-to-metal contact forces.[30] A spring-mass system connected by modal characteristics has been sued to simulate the secondary motion of a skirt.[31] Fang et al. studied the effects of machining surface grooves on piston dynamics.[32]

Finite element analysis (FEA) is a versatile tool to study the mechanical properties of materials. Mechanical behaviour of braided ropes using FEA is shown in Vu et al. and Gerdemeli et al.[33,34] This tool has been used to characterize the motion of skirts. Dursunkaya et al. introduced an elastohydrodynamic model of lubrication to simulate the motion of a skirt.[35] Thermal deformations were calculated using an FEA model of a skirt, in the case of a heavy truck diesel engine skirt. Radial deformations were found to be dependent on engine load. Li et al. analysed the use of FEA to demonstrate the effects of variations in inertia on piston motion and on the friction and lubrication behaviour between a piston skirt and a cylinder liner.[36]

Table 1. Engine specifications.

Component	Rating
Bore	67 mm
Stroke	56 mm
Compression ratio	4.5:1
Power	2.25 kW

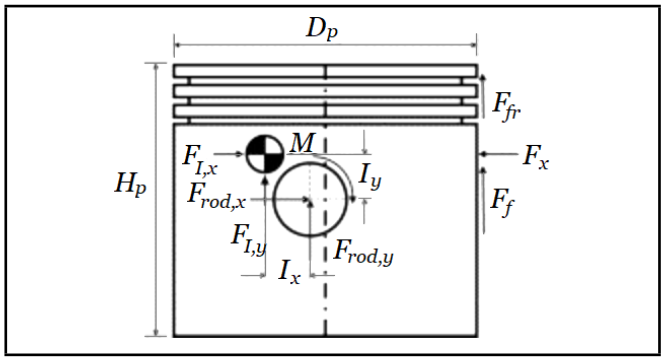

Figure 2. Free body piston diagram.[39]

COMSOL 7 Multiphysics is one of the FEA packages that have been widely used for modelling and simulation.[37] The static Hertz contact model for frictional forces has been verified by using this software package.[38] In the present study, this simulation tool was used to simulate the secondary motion of a KPKN2520 type single cylinder gasoline Kirloskar made engine. Major features of this engine are presented in Table 1.

The novelty of the present work lies in the validation of the proposed model of the lateral motion of the skirt, with results obtained from a COMSOL simulation and the recorded block vibration data. The proposed methodology needs further evaluation, taking into account the influences of oil film lubrication, motion of piston pins, and a selection of various materials for the designing of a skirt.

3. PISTON ASSEMBLY MODEL

3.1. Piston Side-Thrust Force (F_x)

The existence of clearance between the skirt and cylinder liner allows the piston to move and rotate freely within the confined region, resulting in the lateral motion of the skirt and slap. The main driving force is the side-thrust force imparted to the skirt by a connecting rod, as shown in Fig. 2. The skirt has the diameter D_p (mm) and length H_p (mm). The frictional force acting between the rings and liner (F_{fr}), as well as between the liner and skirt (F_f). The contact force of the connecting rod with the skirt is resolved in horizontal ($F_{rod,x}$) and vertical directions ($F_{rod,y}$). Inertial forces are also resolved along the x-axis ($F_{I,x}$), as well as the y-axis ($F_{I,y}$). All forces are expressed in N or kN.

The frictional forces between the piston skirt and cylinder liner, as well as between the rings and liner, act vertically along

the y-axis. The centre of mass of the piston assembly is at the horizontal offset of L_x and at the vertical offset distance of L_y from the connecting rod position.

The force exerted by the connecting rod on the piston pin can be vertically decomposed along the x-axis, as well as the y-axis. As the angle of the connecting rod changes as the piston moves from bottom dead centre (BDC) to top dead centre (TDC), there will be a lateral force pushing the piston on to the cylinder liner. The piston side-thrust force (F_x) takes into consideration both inertial forces as well as gas forces (F_g), as developed by Guzzomi et al.,[40] and is given by the following equation, in terms of the crank radius-connecting rod length ratio (K):

$$F_x = \left[F_g - m_p r\omega^2 \left(\cos(\theta) + K\cos(2\theta)\right)\right]\lambda; \qquad (2)$$

where $\lambda = \frac{K\cos\theta}{\sqrt{1+[\lambda\sin(\theta)]^2}}$, m_p — mass of skirt (kg), θ — crank angle (degree), r — crank radius (mm), ω — angular speed (rad/s).

3.2. Mobility Parameter Determination

Mechanical mobility (M) is defined as the ratio of output velocity of a structure to the excitation force acting on it. Mobility between various input and output points is known as transfer mobility and mobility at a point is often called driving point mobility. This parameter can be used to find the dynamic mass, stiffness, and damping constant of lumped parameter system. The point mobility $M(j\omega)$ expresses the relation between resulting velocity response $V(j\omega)$ and an exciting force $F(j\omega)$, and is given as:[39]

$$M(j\omega)\ [\text{m/N-s}] = \frac{V(j\omega)}{F(j\omega)}; \qquad (3)$$

$$M(j\omega) = \frac{-j\omega\left((K - M\omega^2) + jC\omega\right)}{M\omega^2(K + jC\omega)}. \qquad (4)$$

The mobility measurement was carried out to identify the dynamic properties of the piston and cylinder block. The response of the cylinder block was captured using an accelerometer mounted on the top of the engine block. The response of the symmetric half portion piston skirt was measured using COMSOL 7 FEA software for various cases. One such simulation is depicted in Fig. 3. Tetrahedral elements were used to mesh the quarter part of the skirt. The materials used for this simulation were an aluminium alloy with a density of 2700 kg/m^3, Young's modulus 72 GPa, and Poisson ratio of 0.31.

Data inputs were fed to LABVIEW10 software for post processing. In order to ensure that the simulated results of the behaviour of the piston's secondary motion are comparable and correlated to the actual piston's secondary motion, the mobility was obtained using a running engine under various testing conditions. This was further used to determine the dynamic features of the assembly.

Analysis of the frequency domain plots of mechanical mobility have shown that in the frequency range below the first anti-resonance frequency $\left(\omega_a = \sqrt{\frac{K}{m}}\right)$, the point mobility equation can be approximated as:[39]

$$M(j\omega) = \frac{-j}{m\omega_a}. \qquad (5)$$

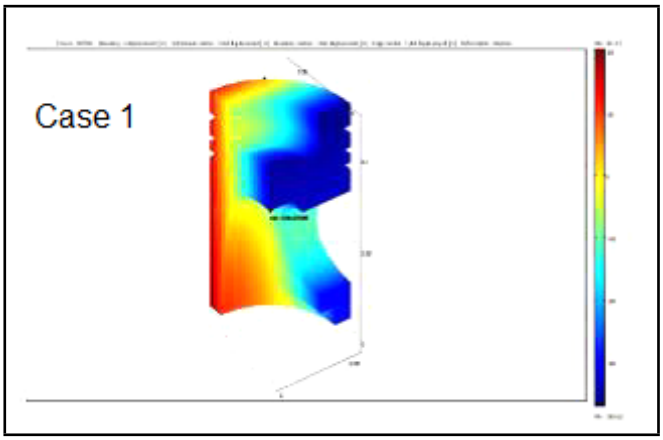

Figure 3. COMSOL Simulation.

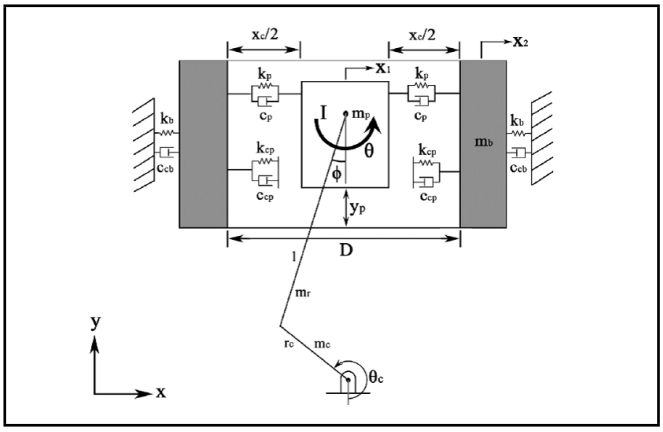

Figure 4. Piston model.[39]

Above the anti-resonance frequency range, the point mobility can be written as:[39]

$$M(j\omega) = \frac{-j\omega_a}{K}. \qquad (6)$$

The above relations were used to find the dynamic mass and stiffness of the skirt, as well as liner system as shown later in Table 3. The interaction between the skirt and cylinder liner of a piston assembly can be modelled as a three degree of freedom system, as shown in Fig. 4. The piston skirt is modelled as a single point with a dynamic mass m_p and moment of inertia (I_p) equal to the corresponding two degrees of freedom (X_p, θ). The cylinder block is modelled as a lumped system having a dynamic mass m_b with a single degree of freedom (X_b), as shown in matrix form in Eq. (2). The piston is located inside the cylinder bore with a nominal clearance of 0.05 mm. The clearance allows the piston to move in the lateral direction and rotate about a piston pin. The clearance between the cylinder and liner X_c is modelled as a mechanical stop in the lateral direction of piston motion with a hard stiffness.

The motion of the system is given by Eq. (7):[39]

$$\begin{bmatrix} m_p & 0 & 0 \\ 0 & m_b & 0 \\ 0 & 0 & I_p \end{bmatrix} \begin{bmatrix} X_p'' \\ X_b'' \\ \theta'' \end{bmatrix} + \begin{bmatrix} C_p & -C_p & 0 \\ -C_p & C_b + C_p & 0 \\ 0 & 0 & C_\theta \end{bmatrix} \begin{bmatrix} X_p' \\ X_b' \\ \theta' \end{bmatrix} + \begin{bmatrix} K_p & -K_p & 0 \\ -K_p & K_b + K_p & 0 \\ 0 & 0 & K_\theta \end{bmatrix} \begin{bmatrix} X_p \\ X_b \\ \theta \end{bmatrix} = \begin{bmatrix} F_x \\ 0 \\ M_z \end{bmatrix}; \qquad (7)$$

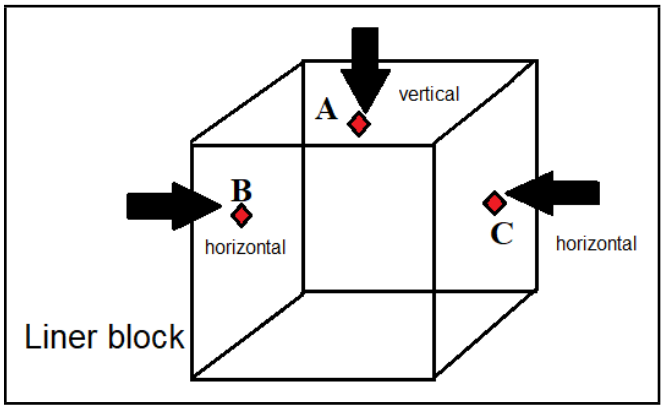

Figure 5. Accelerometer locations.

Table 2. Testing conditions.

Case	RPM	Load
1	2000	100%
2	2000	80%
3	3000	80%
4	3000	100%
5	3000	(motored)

where m_p — dynamic mass of skirt (kg), m_b — dynamic mass of block (kg), I_p — inertia of piston (kg-m^2), C_p — dynamic damping coefficient of skirt (N-s/m), K_p — dynamic stiffness coefficient of skirt (N/m), C_b — dynamic damping coefficient of block (N-s/m), K_b — dynamic stiffness coefficient of block (N/m), F_x — side-thrust force (N), M_z — net moment (N-m).

3.3. Experimental Setup

The block vibrations were measured by means of a Wilcox-type mono-axial accelerometer, which was mounted in vertical (A) and horizontal orientations (B, C) on the engine block (Fig. 5). During the tests, engine speeds and loading conditions were varied, as seen in Table 2.

4. RESULTS AND DISCUSSION

Figures 6 and 7 show the plot of the piston's side-thrust force at 2000 RPM and 3000 RPM conditions. Positive values of force means contact towards thrust side of the skirt, whereas negative values predict contact towards the anti-thrust side. Peak values were observed during the expansion stroke. At zero values, the inertial forces acting on the skirt balance the gas forces on its top crown. As seen from these plots, side-thrust force changes its direction five times in a complete engine cycle, indicating instances of piston slapping contact as depicted by circles.

COMSOL 7 software was then used to simulate piston secondary motion, and hence compute the lateral piston velocity as shown in Figs. 8 and 9.

The lateral velocity of the skirt was seen in a range from -20 to 20 m/s. It falls with an increase in engine loading values. Negative values of lateral velocity show clockwise tilting of the skirt, whereas the positive values predict an anti-clockwise tilt. Major changes were seen during suction and compression strokes. The velocity of piston approaches zero values near the top dead centre positions. Piston mobility was computed for the given testing conditions, as depicted in Figs. 10 and 11, from values of lateral velocity of the skirt obtained using a COMSOL model (Figs. 8 and 9).

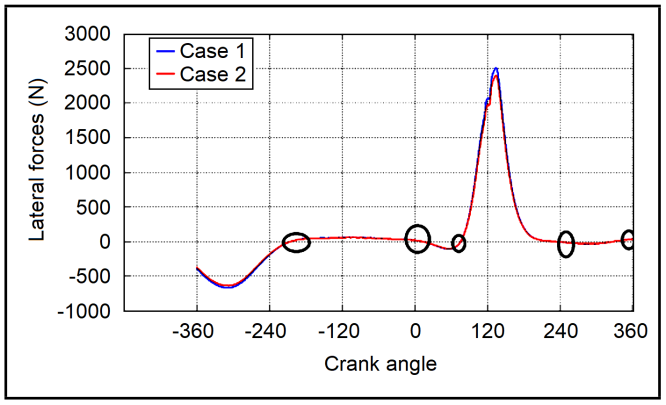

Figure 6. Representation of piston side-thrust force (2000 RPM).

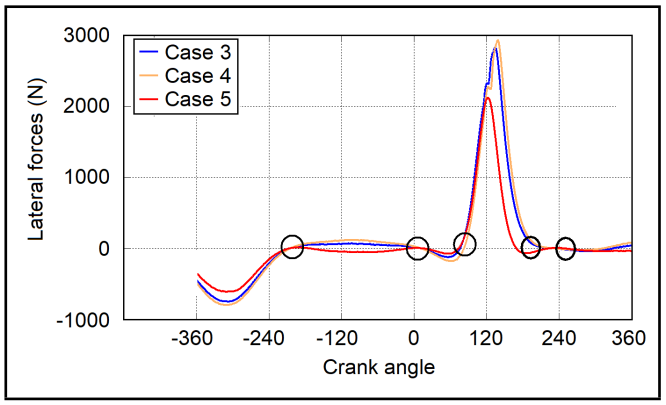

Figure 7. Representation of piston side-thrust force (3000 RPM).

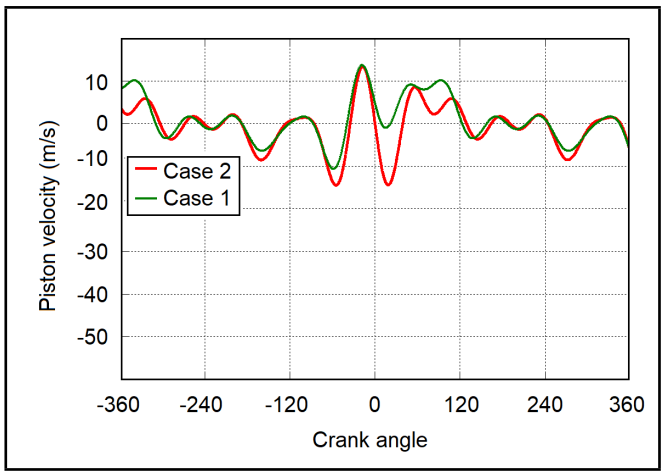

Figure 8. Representation of piston lateral velocity (2000 RPM).

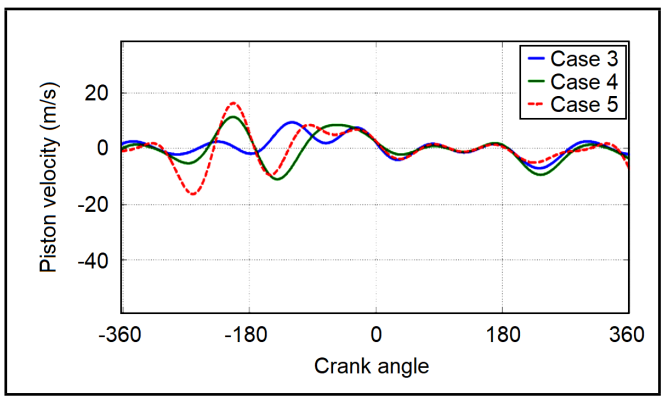

Figure 9. Representation of piston lateral velocity (3000 RPM).

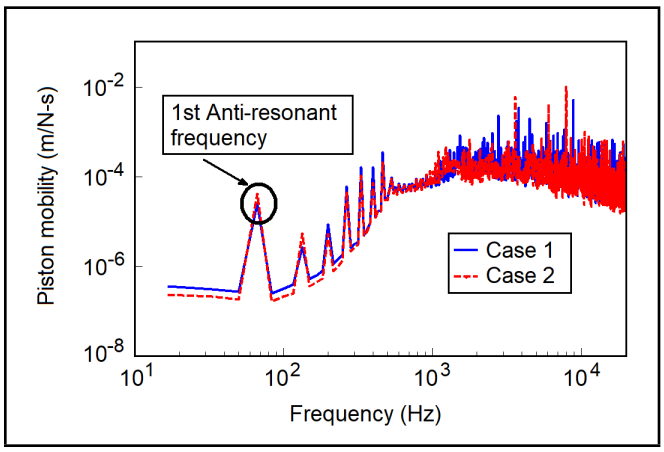

Figure 10. Representation of piston mobility (2000 RPM).

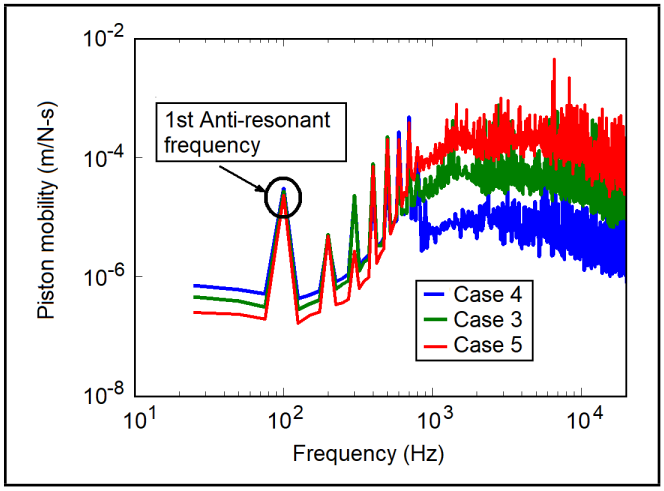

Figure 11. Representation of piston mobility (3000 RPM).

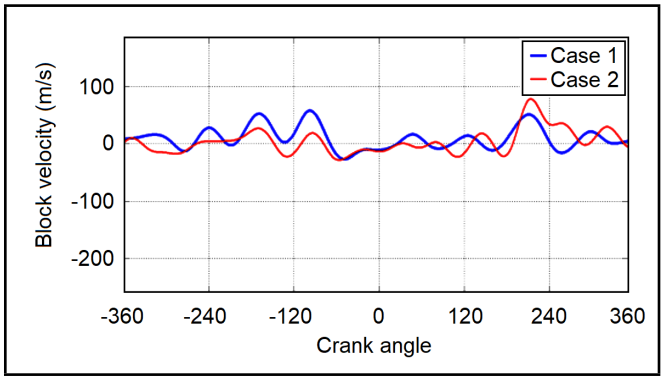

Figure 12. Representation of block velocity (2000 RPM).

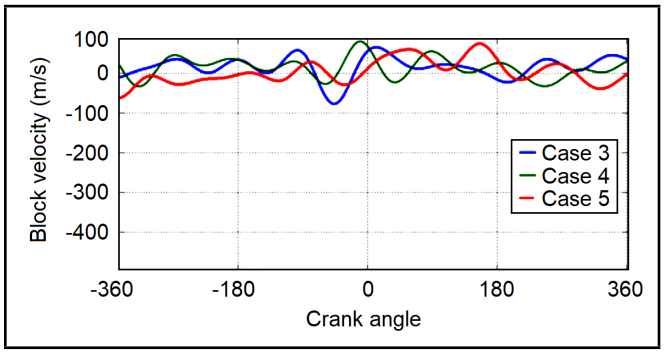

Figure 13. Representation of block velocity (3000 RPM).

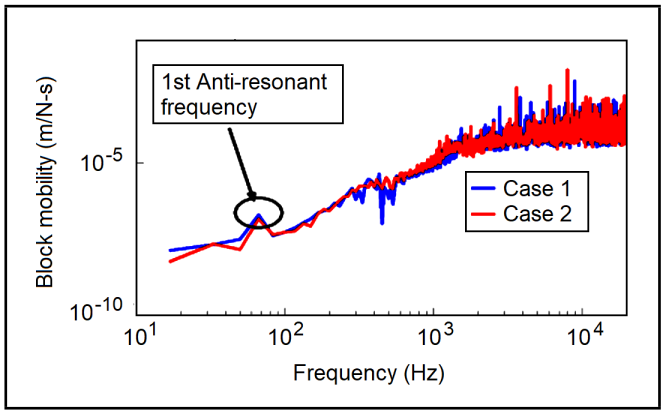

Figure 14. Representation of block mobility (2000 RPM).

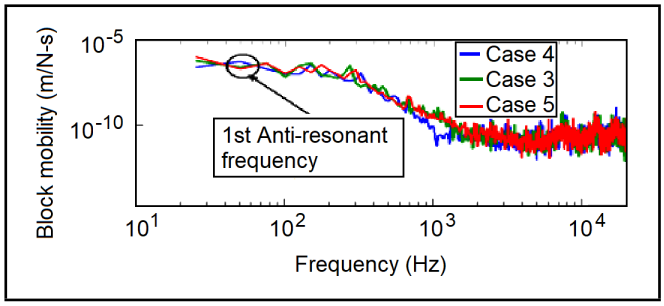

Figure 15. Representation of block mobility (3000 RPM).

Similarly, mobility for the cylinder block was found (Figs. 14 and 15) using the numerical integration of the accelerometer data (in a vertical position), which gives values of the lateral block vibration velocity (Figs. 12 and 13). Lateral block velocities were found to be in range of -100 m/s to 100 m/s, and were found to increase with engine speed.

Values of the first anti-resonant frequencies were found to be over 50 Hz. The curve for piston mobility had sharp and dense peaks, as compared to engine block mobility. This is because the skirt is in direct contact with intense gas forces, whereas the engine block acts as a nonlinear and time-dependent attenuator for these forces. Using the concept of anti-resonant frequency as discussed in the previous sections, the various dynamic parameters of a liner-piston system were computed for the given test conditions. The results can be seen in Table 3.

The rotational motion of the skirt was simulated by solving dynamic equations of motion and comparing with the results obtained from COMSOL as seen in Figs. 16–20. Both of the trends showed a good correlation. The tilting of the skirt was found to be in the range of $-0.2°$ to $0.2°$. Positive values of tilting angle means a tilt towards thrust side, whereas the negative values imply a tilt towards anti-thrust side of the liner. Peak values of tilting were seen during the expansion and exhaust strokes. As seen from the figures, the tilt angle of the piston changes its direction at both dead centres. The piston is predicted to slide for some duration before TDC along the cylinder liner. The piston's tilt angle was seen to decrease with the increase of load, as well as with speed.

Figures 21–25 show the simulated and measured vibratory response of the cylinder block as captured by the accelerometer. The trends in the simulated vibration response of the cylinder block show a good agreement with the measured vibration response in ranges of 3–4 mm. In these figures, the impact of the piston on the cylinder wall results in a sudden increase

Table 3. Dynamic parameters of system.

Test Case	Parameter Value	
	Piston Parameter	**Liner Parameter**
1	$\omega_a = 65$ Hz $[M(J\omega)]_{\omega_a} =$ $2.5 * 10^{-5}$ m/N-s $c = 109330$ kg/s $k = 1.63 * 10^7$ kg/s^2 $m = 63$ kg	$\omega_a = 67$ Hz $[M(J\omega)]_{\omega_a} =$ 10^{-7} m/N-s $c = 42884$ kg/s $k = 4.2 * 10^9$ kg/s^2 $m = 23754$ kg
2	$\omega_a = 65$ Hz $[M(J\omega)]_{\omega_a} =$ $3.98 * 10^{-5}$ m/N-s $c = 109330$ kg/s $k = 1 * 10^7$ kg/s^2 $m = 39$ kg	$\omega_a = 67$ Hz $[M(J\omega)]_{\omega_a} =$ 10^{-7} m/N-s $c = 42884$ kg/s $k = 4.2 * 10^9$ kg/s^2 $m = 23754$ kg
3	$\omega_a = 100$ Hz $[M(J\omega)]_{\omega_a} =$ $3.1623 * 10^{-5}$ m/N-s $c = 172750$ kg/s $k = 1.98 * 10^7$ kg/s^2 $m = 50$ kg	$\omega_a = 63$ Hz $[M(J\omega)]_{\omega_a} =$ $1.99 * 10^{-7}$ m/N-s $c = 69669$ kg/s $k = 1.98 * 10^9$ kg/s^2 $m = 11937$ kg
4	$\omega_a = 100$ Hz $[M(J\omega)]_{\omega_a} =$ $2.5 * 10^{-5}$ m/N-s $c = 172750$ kg/s $k = 2.5 * 10^7$ kg/s^2 $m = 63$ kg	$\omega_a = 63$ Hz $[M(J\omega)]_{\omega_a} =$ $2.5 * 10^{-7}$ m/N-s $c = 69669$ kg/s $k = 1.5 * 10^9$ kg/s^2 $m = 10105$ kg
5	$\omega_a = 100$ Hz $[M(J\omega)]_{\omega_a} =$ $1.9 * 10^{-5}$ m/N-s $c = 172750$ kg/s $k = 3.3 * 10^7$ kg/s^2 $m = 83$ kg	$\omega_a = 63$ Hz $[M(J\omega)]_{\omega_a} =$ $2.5 * 10^{-7}$ m/N-s $c = 69669$ kg/s $k = 1.63 * 10^9$ kg/s^2 $m = 10105$ kg

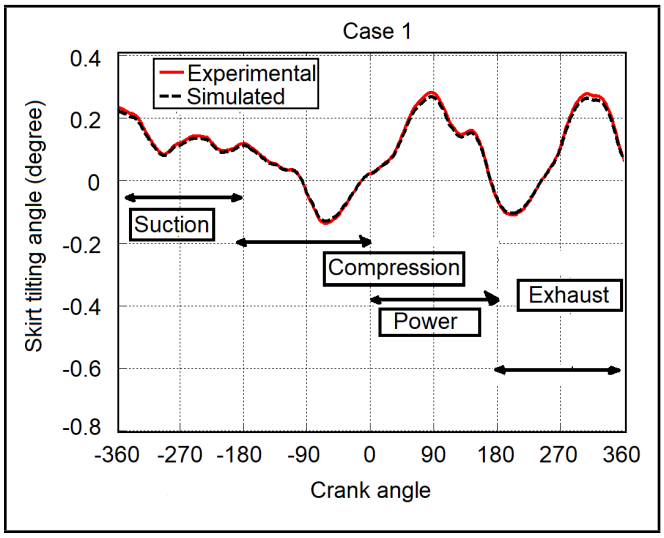

Figure 16. Representation of tilting motion (2000 RPM—80% load).

of the vibration amplitude and this is clearly marked in the diagram where a few impacts occurs. The induced vibration amplitude of the cylinder block measured experimentally is slightly higher than the predicted induced vibration amplitude. This is due to several other contributing sources, like mechanical noises that add to the actual vibration data recorded.

The induced vibrations of the block increase with engine speed, whereas the sliding duration falls with an increase in velocity. This is due to higher impact force and acceleration generated during the piston slap and a higher reaction impact force from the liner. The effects of load and speed variations on piston lateral motion are seen in Figs. 26 and 27. As the speed of engine increases, the side-thrust force, which is dependent upon speed, also increases. An increase in the magnitude of

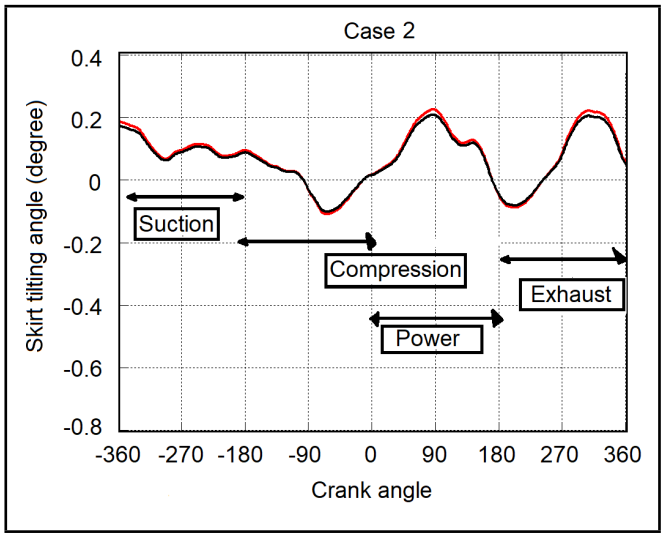

Figure 17. Representation of tilting motion (2000 RPM—100% load).

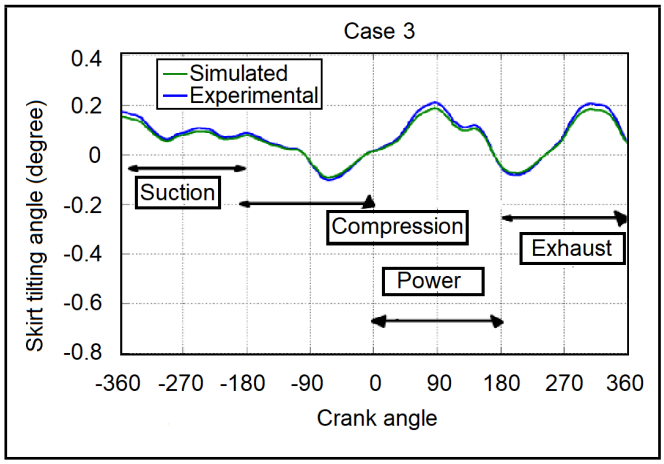

Figure 18. Representation of tilting motion (3000 RPM—motored).

this side-thrust force acting on the piston results in the piston bouncing off the liner more frequently for longer durations and the sliding duration of the piston skirt along the liner falls. At low engine speeds, the vibration response of the cylinder block induced by the slapping contact of the piston has a longer duration till decay, as compared with higher engine speeds.

5. CONCLUSIONS

Noise emission from engines are the results of several contributing resources, out of which mechanical noise is a major contributor. Lateral motion of the skirt is a major contributor in motion-based noise. There have been several numerical models that were proposed to study this motion. This work discusses one such two-dimensional modal model of piston secondary motion. Various dynamic parameters of the system were calculated using the concept of mobility. These parameters were used to generate profiles of piston secondary motion, resulting in block vibrations and the tilting angle of skirt. The effects of variations in various engine operational parameters were also analysed. These calculated values were compared with simulated values obtained from the COMSOL 7 software tool, which validate the model. The sliding motion of the piston along the liner was observed to increase, with an increase in load and speed, which is in agreement with the previous data

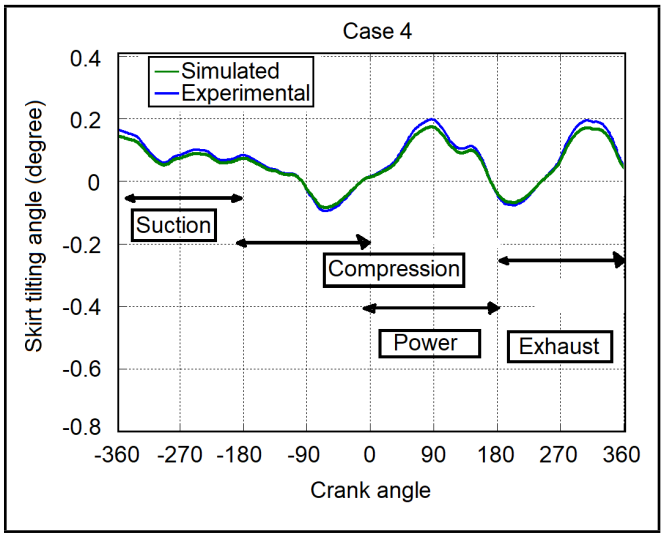

Figure 19. Representation of tilting motion (3000 RPM—80% load).

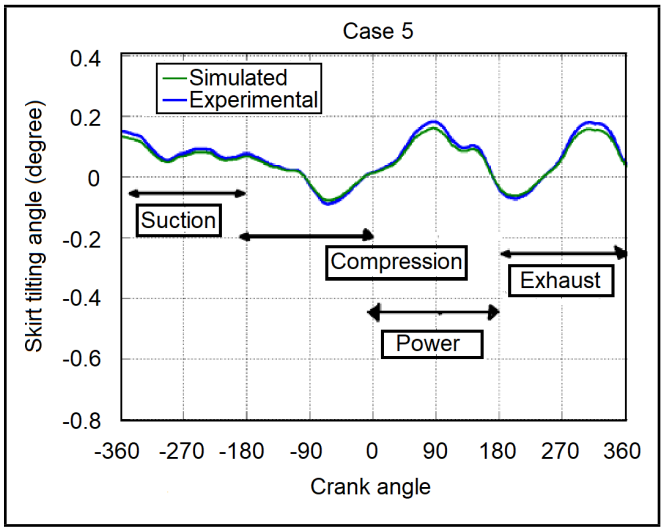

Figure 20. Representation of tilting motion (3000 RPM—100% load).

available.[41] In future work, the lateral motion of skirt should also takes into account the profile of the skirt, thermal deformations, and lubrication dynamics.

REFERENCES

[1] Cho, S., Ahn, S., and Kim, Y. A simple model to estimate the impact force induced by piston slap, *Journal of Sound and Vibrations*, **255** (2), 229–242, (2002). https://dx.doi.org/10.1006/jsvi.2001.4152

[2] He, Z., Xie, W., Zhang, G., Hong, Z., and Zhang, J. Piston dynamic characteristics analyses based on FEM method Part I: Effected by piston skirt parameters, *Advances in Engineering Software*, **75**, 68–85, (2014). https://dx.doi.org/10.1016/j.advengsoft.2014.05.003

[3] Meng, X. and Xie, Y. A new numerical analysis for piston skirt-liner system lubrication considering the effects of connecting rod inertia, *Tribology International*, **47**, 235–253, (2012). https://dx.doi.org/10.1016/j.triboint.2011.12.013

[4] Tan, Y.-C. and Ripin, Z. M. Analysis of piston secondary motion, *Journal of Sound and Vibration*, **332** (20), 5162–5176, (2013). https://dx.doi.org/10.1016/j.jsv.2013.04.042

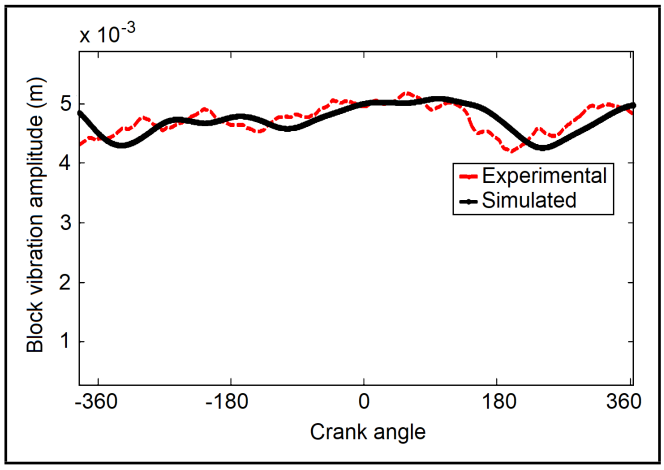

Figure 21. Effect of engine speed on block vibrations (2000 RPM—80% load).

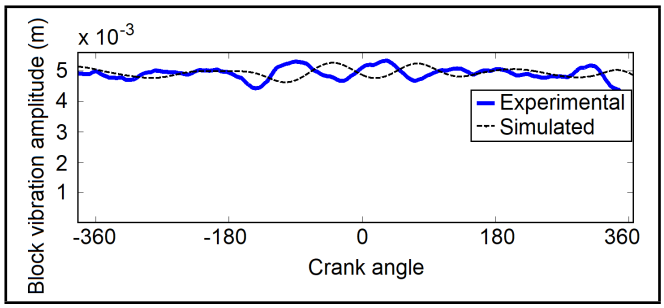

Figure 22. Effect of engine speed on block vibrations (2000 RPM—100% load).

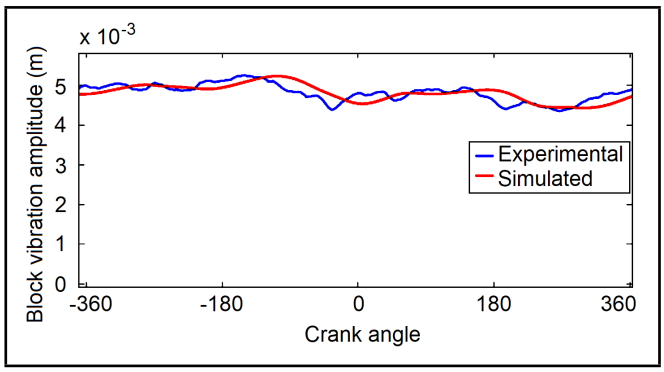

Figure 23. Effect of engine speed on block vibrations (3000 RPM—motored).

[5] Chen, J. and Randall, R. B. Vibration signal processing of piston slap and bearing knock in IC engines, *Proceedings of Surveillance 6*, (2011).

[6] Meng, X., Fang, C., and Xie ,Y., Transient tribodynamic model of piston skirt-liner systems with variable speed effects, *Tribology International*, **94**, 640–651, (2016). https://dx.doi.org/10.1016/j.triboint.2015.10.034

[7] Zhao, B., Dai, X., Zhang, Z., and Xie, Y. A new numerical method for piston dynamics and lubrication analysis, *Tribology International*, **94**, 395–408, (2016). https://dx.doi.org/10.1016/j.triboint.2015.09.037

[8] Dolatabadi, N., Littlefair, B., DelaCruz, M., Theodossiades, S., Rothberg, S., and Rahnejat, H. A transient tribodynamic approach for the calculation of internal combustion engine piston slap noise, *Jour-*

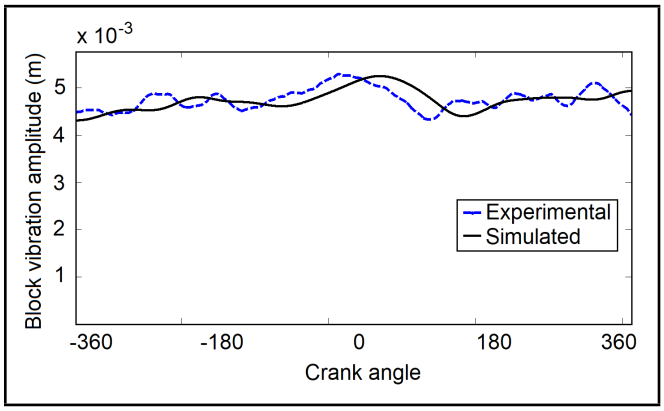

Figure 24. Effect of engine speed on block vibrations (3000 RPM—80% load).

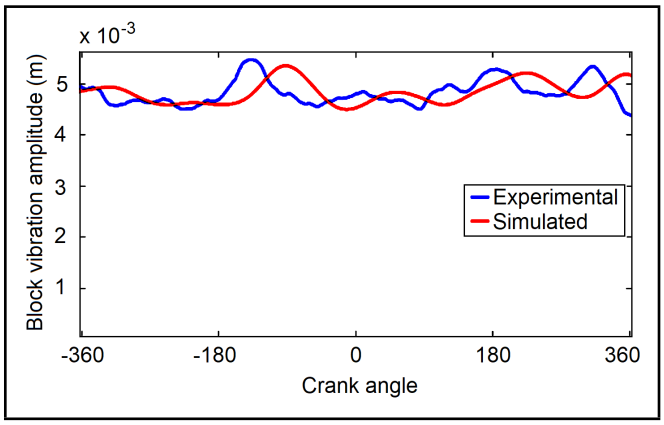

Figure 25. Effect of engine speed on block vibrations (3000 RPM—100% load).

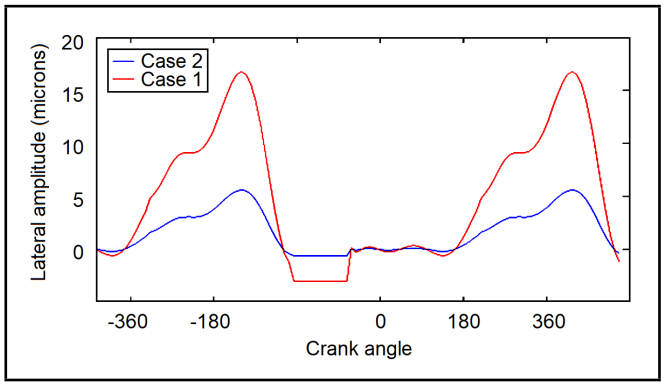

Figure 26. Effect of engine speed on lateral motion (2000 RPM).

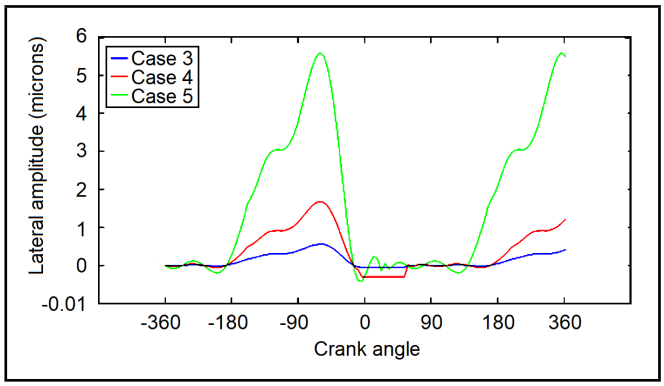

Figure 27. Effect of engine speed on lateral motion (3000 RPM).

nal of Sound and Vibration, **352**, 192–209, (2015). https://dx.doi.org/10.1016/j.jsv.2015.04.014

[9] Han, D. C. and Lee, J. S. Analysis of the piston ring lubrication with a new boundary condition, *Tribology International*, **31** (12), 753–760, (1998). https://dx.doi.org/10.1016/S0301-679X(98)00096-6

[10] Flores, P., Ambrósio, J., Claro, J., and Lankarani, H. Translational joints with clearance in rigid multi body systems, *Journal of Computational and Nonlinear Dynamics*, **3** (1), 011007, (2008). https://dx.doi.org/10.1115/1.2802113

[11] Cho, S. H., Ahn, S. T., and Kim, Y. H. A simple model to estimate the impact force induced by piston slap, *Journal of Sound and Vibration*, **255** (2), 229–242, (2002). https://dx.doi.org/10.1006/jsvi.2001.4152

[12] Rahnejat, H., Balakrishnan, S., King, P., and Howell-Smith, S. In-cylinder friction reduction using a surface finish optimization technique, *Proceedings of the Institution of Mechanical Engineers, Part D: Journal of Automobile Engineering*, **220** (9), 1309–1318, (2006). https://dx.doi.org/10.1243/09544070JAUTO282

[13] Flores, P., Leine, R., and Glocker, C. Modeling and analysis of planar rigid multibody systems with translational clearance joints based on the non-smooth dynamics approach, *Multibody System Dynamics*, **23** (2), 165–190, (2010). https://dx.doi.org/10.1007/s11044-009-9178-y

[14] Zhang, Z., Xie, Y., Zhang, X. and Meng, X. Analysis of piston secondary motion considering the variation in the system inertia, *Proceedings of the Institution of Mechanical Engineers, Part D: Journal of Automobile Engineering*, **223** (4), 549–563, (2009). https://dx.doi.org/10.1243/09544070JAUTO1078

[15] Farahanchi, F. and Shaw, S. W. Chaotic and periodic dynamics of a slider-crank mechanism with slider clearance, *Journal of Sound and Vibration*, **177** (3), 307–324, (1994). https://dx.doi.org/10.1006/jsvi.1994.1436

[16] McFadden, P. D. and Turnbull, S. R. Dynamic analysis of piston secondary motion in an internal combustion engine under non-lubricated and fully flooded lubricated conditions, *Proceedings of the Institution of Mechanical Engineers, Part C: Journal of Mechanical Engineering Science*, **225** (11), 2575–2585, (2011). https://dx.doi.org/10.1177/0954406211408674

[17] Geng, Z. and Chen, J. Investigation into piston-slap-induced vibration for engine condition simulation and monitoring, *Journal of Sound and Vibration*, **282** (3–5), 735–751, (2005). https://dx.doi.org/10.1016/j.jsv.2004.03.057

[18] Kim, T. J. Numerical analysis of the piston secondary dynamics in reciprocating compressors, *Journal of Mechanical Science and Technology*, **17** (3), 350–356, (2003). https://dx.doi.org/10.1007/BF02984361

[19] Liu, K., Xie, Y. B., and Gui, C. L. A comprehensive study of the friction and dynamic motion of the piston assembly, *Proceedings of the Institution of Mechanical Engineers,*

Part J: Journal of Engineering Tribology, **212** (3), 221–226, (1998). https://dx.doi.org/10.1243/1350650981542038

[20] Offner, G., Herbst, H. M., and Priebsch, H. H. A methodology to simulate piston secondary movement under lubricated contact conditions, SAE Technical Paper 2001-01-0565, (2001). https://dx.doi.org/10.4271/2001-01-0565

[21] Comfort, A. An introduction to heavy-duty diesel engine frictional losses and lubricant properties affecting fuel economy-Part I, SAE Technical Paper 2003-01-3225, (2003). https://dx.doi.org/10.4271/2003-01-3225

[22] Ruggiero, A. and Senatore, A. Computer model for the prediction of the impact force induced by piston slap in internal combustion engines, *The Annals of the University of "Dunărea de Jos" of Galaţi, Fascicle VIII: Tribology*, (2003).

[23] Desai, H. Computer aided kinematic and dynamic analysis of a horizontal slider crank mechanism used for single-cylinder four stroke internal combustion engine, *Proceedings of the World Congress on Engineering*, London, U. K., (2009).

[24] Wilson, R. and Fawcett, J. N. Dynamics of the slider-crank mechanism with clearance in the sliding bearing, *Mechanism and Machine Theory*, **9** (1), 61–80, (1974). https://dx.doi.org/10.1016/0094-114X(74)90008-1

[25] Haddad, S. D. and Tjan, K. T. An analytical study of offset piston and crankshaft designs and the effect of oil film on piston slap excitation in a diesel engine, *Mechanism and Machine Theory*, **30** (2), 271–284, (1995). https://dx.doi.org/10.1016/0094-114X(94)00035-J

[26] McNally, C. P. Development of a numerical model of piston secondary motion for internal combustion engines, Master's thesis, Massachusetts Institute of Technology, (2000). https://dspace.mit.edu/bitstream/handle/1721.1/26880/46310081-MIT.pdf?sequence=2

[27] Livanos, G. A. and Kyrtatos, N. P. Friction model of a marine diesel engine piston assembly, *Tribology International*, **40** (10–12), 1441–1453, (2007). https://dx.doi.org/10.1016/j.triboint.2007.01.020

[28] Mansouri, S. H. and Wong, V. W. Effects of piston design parameters on piston secondary motion and skirt-liner friction, *Proceedings of the Institution of Mechanical Engineers, Part J: Journal of Engineering Tribology*, **219** (6), 435–449, (2005). https://dx.doi.org/10.1243/135065005X34026

[29] Lu, Y., Li, S., Wang, P., Liu, C., Zhang, Y., and Müller, N. The analysis of secondary motion and lubrication performance of piston considering the piston skirt profile, *Shock and Vibration*, **2018**, 1–27, (2018). https://dx.doi.org/10.1155/2018/3240469

[30] Gunelsu, O. and Akalin, O. Development of a piston secondary motion model for skirt friction analysis, *ASME 2012 Internal Combustion Engine Division Fall Technical Conference*, Vancouver, Canada, (2012). https://dx.doi.org/10.1115/ICEF2012-92166

[31] Koizumi, T., Tsujiuchi, N., Okamura, M., Tsukijima, H., Kubomoto, I., and Ishida, E. Reduction of piston slap excitation by optimizing piston profiles, retrieved from: https://pdfs.semanticscholar.org/3ed8/bc13ed23fc877fd65eabe31477004a3990e3.pdf

[32] Fang, C., Meng, X., and Xie, Y. A piston tribodynamic model with deterministic consideration of skirt surface grooves, *Tribology International*, **110**, 232–251, (2017). https://dx.doi.org/10.1016/j.triboint.2017.02.026

[33] Vu, T. D., Durville, D., and Davies, P. Finite element simulation of the mechanical behavior of synthetic braided ropes and validation on a tensile test, *International Journal of Solids and Structures*, **58**, 106–116, (2015). https://dx.doi.org/10.1016/j.ijsolstr.2014.12.022

[34] Gerdemeli, I., Kurt, S., and Anil, A. S. Analysis with finite element method of wire rope, retrieved from: http://meching.com/journal/Archive/2012/11/185_Kurt.pdf

[35] Dursunkaya, Z., Keribar, R., and Ganapathy, V. A model of piston secondary motion and elastohydrodynamic skirt lubrication, *Journal of Tribology*, **116** (4), 777–785, (1994). https://dx.doi.org/10.1115/1.2927332

[36] Li, G., Gu, F., Wang, T., Yang, T., and Ball, A. Investigation into the dynamic response of cylinder liners in an IC engine based on a validated finite-element model, *Systems Science & Control Engineering*, **5** (1), 56–69, (2018). https://dx.doi.org/10.1080/21642583.2016.1277565

[37] COMSOL Multiphysics, Major news in COMSOL software version 5.3a, retrieved from: https://www.comsol.com/release/5.3a

[38] Pennec, F., Achkar, H., Peyrou, D., Plana, R., Pons, P., and Courtade, F. Verification of contact modelling with COMSOL multiphysics software, Rapport LAAS n°07604, (2007). https://hal.archives-ouvertes.fr/hal-00180257/document

[39] Tan, Y.-C. and Ripi, Z. M. Analysis of piston secondary motion, *Journal of Sound and Vibration*, **332** (20), 5162–5176, (2013). https://dx.doi.org/10.1016/j.jsv.2013.04.042

[40] Guzzomi, A. L., Hesterman, D. C., and Stone, B. J. Variable inertia effects of an engine including piston friction and a crank or gudgeon pin offset, *Proceedings of the Institution of Mechanical Engineers, Part D: Journal of Automobile Engineering*, **222** (3), 397–414, (2008). https://dx.doi.org/10.1243/09544070JAUTO590

[41] Tan, Y.-C. and Ripin, Z. M. Technique of measuring piston secondary motion using laser displacement sensors, *Experimental Mechanics*, **52** (9), 1447–1459, (2012). https://dx.doi.org/10.1007/s11340-012-9600-x